Nuclear Engineering and Technology 50 (2018) 18–24

Contents lists available at ScienceDirect

Nuclear Engineering and Technology

journal homepage: www.elsevier.com/locate/net

Original Article

Compound effects of operating parameters on burnup credit criticality analysis in boiling water reactor spent fuel assemblies

Shang-Chien Wu [a], Der-Sheng Chao [b], Jenq-Horng Liang [a, *]

[a] Institute of Nuclear Engineering and Science, National Tsing Hua University, Hsinchu 30013, Taiwan, ROC
[b] Nuclear Science and Technology Development Center, National Tsing Hua University, Hsinchu 30013, Taiwan, ROC

ARTICLE INFO

Article history:
Received 8 June 2017
Received in revised form
5 September 2017
Accepted 19 September 2017
Available online 11 November 2017

Keywords:
Burnup Credit
BWR
Compound Effects
Effective Multiplication Factor
Nuclear Criticality Safety Analysis

ABSTRACT

This study proposes a new method of analyzing the burnup credit in boiling water reactor spent fuel assemblies against various operating parameters. The operating parameters under investigation include fuel temperature, axial burnup profile, axial moderator density profile, and control blade usage. In particular, the effects of variations in one and two operating parameters on the curve of effective multiplication factor (k_{eff}) versus burnup (B) are, respectively, the so-called single and compound effects. All the calculations were performed using SCALE 6.1 together with the Evaluated Nuclear Data Files, part B (ENDF/B)-VII238-neutron energy group data library. Furthermore, two geometrical models were established based on the General Electric (GE)14 10 × 10 boiling water reactor fuel assembly and the Generic Burnup-Credit (GBC)-68 storage cask. The results revealed that the curves of k_{eff} versus B, due to single and compound effects, can be approximated using a first degree polynomial of B. However, the reactivity deviation (or changes of k_{eff}, Δk) in some compound effects was not a summation of the all Δk resulting from the two associated single effects. This phenomenon is undesirable because it may to some extent affect the precise assessment of burnup credit. In this study, a general formula was thus proposed to express the curves of k_{eff} versus B for both single and compound effects.

1. Introduction

Nuclear criticality safety analysis is essential for ensuring the safe storage, transportation, reprocessing, and disposition of spent fuel. Traditionally, the analysis is based on the most conservative condition in which all the spent fuel assemblies have the most reactive nuclide inventories. For example, both pressurized water reactors and boiling water reactors (BWRs) use the condition of fresh fuel assemblies. BWRs especially use the condition of reactivity peak if the fuel assemblies contain gadolinium (Gd) rods. The advantages of such assumptions simplify nuclear criticality safety analysis while reducing computation time. However, one disadvantage of such assumptions is that, to maintain nuclear criticality safety, there is less spent fuel storage capacity, which subsequently creates an economic issue [1–6]. Therefore, the usage of burnup credit to minimize this problem is an appealing option.

When performing nuclear criticality safety analysis, the concept of burnup credit involves using credit to reduce the reactivity caused by the irradiation of nuclear fuel during power operation [4]. The reactivity reduction includes the consumption of fissile materials as well as the production of strong neutron-absorbed materials, such as actinides and fission products. As a whole, the motivation for considering burnup credit can be summarized as follows [4]: (1) capacity improvement in spent fuel storage facilities can avoid or minimize adverse environmental damage associated with new storage pools, dry storage facilities, and reprocessing facilities; (2) use of higher capacity casks can lead to fewer shipments, less exposure to workers and public, and lower risk possibility of radiological accidents; and (3) for the disposal of spent fuel assemblies, the utilization of higher capacity casks can enhance the efficiency of spent fuel storage, thus implying that a smaller repository footprint is possible. Therefore, an inclusion of burnup credit in nuclear criticality safety analysis is of vital importance.

In reality, reactor operating history affects spent fuel composition by changing the depletion rate of uranium and the generation rates of plutonium, fission products, or other actinides [2]. In examining the effects of such reactor operating history

* Corresponding author.
E-mail address: jhliang@ess.nthu.edu.tw (J.-H. Liang).

https://doi.org/10.1016/j.net.2017.09.004

on burnup credit criticality analysis in BWR spent fuel assemblies, this study considers the most important operating parameters in reactor operating history, namely, fuel temperature (FT), axial burnup profile (AB), axial moderator density profile (AM), and control blade usage (CB) [2]. Furthermore, to our knowledge, there has been a lack of studies that have analyzed compound effects in regard to the characteristics of effective multiplication factor (k_{eff}) versus burnup (B) resulting from simultaneous variations of two operating parameters. Therefore, such analysis is the objective of this study. The relative importance of both major and minor actinides as well as fission products in the characteristics of k_{eff} versus B due to both single and compound effects are also investigated in detail.

2. Calculation models and method

In this study, all the calculations were performed using the SCALE 6.1 computer code together with the Evaluated Nuclear Data Files, part B (ENDF/B)-VII 238-neutron energy group data library [7]. The SCALE computer code was developed by the Oak Ridge National Laboratory (ORNL) and has been widely used for decades to perform nuclear criticality safety analyses. The SCALE 6.1 computer code comprises various multipurpose control modules. In the calculation procedures conducted in this study, TRITON was first used to perform two-dimensional depletion calculations to generate ORIGEN-ARP libraries. These ORIGEN-ARP libraries contain the atomic densities of spent fuel inventories under prescribed levels of initial fuel enrichment and moderator density. Subsequently, the STARBUCS control module utilized these ORIGEN-ARP libraries along with the requested operating parameters to quickly calculate burned fuel composition. In addition, if the axial burnup or moderator density profile was considered in the calculation, the ORIGEN-ARP libraries were used 25 times to generate burned fuel composition for each axial zones in the fuel assembly, and thus a three-dimensional model of the fuel assembly was established. Finally, the burned fuel was inserted into the CSAS5 control module to calculate k_{eff} by means of a 3-D Monte Carlo criticality calculation model.

Two geometrical models representing the typical General Electric (GE)14 10 × 10 BWR fuel assembly and General Burnup Credit (GBC)-68 storage cask (including 68 BWR spent fuel assemblies) [1,2] were adopted in this study and are shown in Fig. 1A and B, respectively. The fuel assembly is composed of two water rods and 92 fuel rods. A total of 68 fuel assemblies are placed in the cask. The fuel rod pitch, active fuel length, and outer dimension of the fuel channel are 1.295, 381, and 13.914 cm, respectively. The fuel rods, with a height of 381 cm, were divided into 25 axial zones if nonuniform axial burnup or moderator density profile was considered in the calculations, but otherwise only one axial zone was applied. Notably, this study followed the approaches by Nuclear Regulatory Commission (NRC)/ORNL for using BWR fuel assemblies that did not contain Gd [2]. The initial enrichment of the fuel rods in all the fuel assemblies was 5 w/o. The fuel, cladding, and moderator temperatures were 840, 567, and 512 K, respectively. The power density (or specific power) during the power operation was maintained at 30 MW/MTU, and the cooling time was 5 years. A total of 28 nuclides were tracked and included: (1) 9 major actinides (i.e., ^{234}U, ^{235}U, ^{238}U, ^{238}Pu, ^{239}Pu, ^{240}Pu, ^{241}Pu, ^{242}Pu, and ^{241}Am); (2) 3 minor actinides (i.e., ^{236}U, ^{237}Np, ^{243}Am); and (3) 16 major fission products (i.e., ^{95}Mo, ^{99}Tc, ^{101}Ru, ^{103}Rh, ^{109}Ag, ^{133}Cs, ^{147}Sm, ^{149}Sm, ^{150}Sm, ^{151}Sm, ^{152}Sm, ^{143}Nd, ^{145}Nd, ^{151}Eu, ^{153}Eu, ^{155}Gd). The selection of these nuclides followed the recommendations of the US NRC [1,2]. The standard deviation of k_{eff} is approximately 10 pcm for all the calculations performed in this study.

Four important operating parameters were considered in this study, including FT, AM, AB, and CB. Only two variations in all the operating parameters were considered in this study and are shown in Table 1. In addition, for simplicity, certain approaches were used to assume these operating conditions, which will be described in detail in the following section. Furthermore, six combinations resulted when any two out of four operating parameters were selected simultaneously. These are listed in Table 2. Notably, the reference conditions employed in this study for the reactivity deviation (or change of k_{eff}, Δk) calculations consisted of FT = 840 K, AM = uniform, AB = uniform, and CB = full withdrawal. The uniform and nonuniform profiles of axial burnup and moderator density employed are shown in Fig. 2A and B, respectively. These profiles were adopted from assembly B2 of the LaSalle Unit 1 Commercial Reactor Critical (CRC) data and NRC/ORNL document and have been widely accepted for burnup credit calculations [2,8].

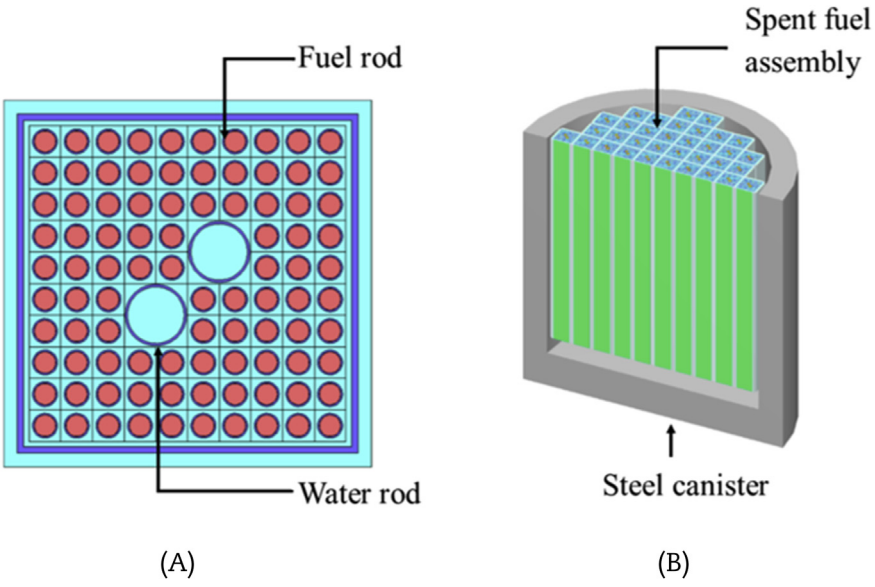

Fig. 1. Geometrical models. (A) GE 10 × 10 fuel assembly model. (B) GBC-68 cask model.

Table 1
Conditions of operating parameters and definition of reactivity deviation corresponding to each operating parameter.

Operating parameter	Reference condition	Test condition	Reactivity deviation
Fuel temperature	840 K	1140 K	$\Delta k_{FT} = k_{1140} - k_{ref}$
Axial burnup profile	Uniform (Fig. 2)	Nonuniform (Fig. 2)	$\Delta k_{AB} = k_{\text{nonuniform AB}} - k_{ref}$
Axial moderator density profile	Uniform (Fig. 2)	Nonuniform (Fig. 2)	$\Delta k_{AM} = k_{\text{nonuniform AM}} - k_{ref}$
Control blade usage	Full withdrawal	Full insertion	$\Delta k_{CB} = k_{\text{full insertion}} - k_{ref}$

Table 2
Types of compound effects and definition of reactivity deviation corresponding to each type of compound effects.

Type	Operating parameter				Reactivity deviation
	FT	AB	AM	CB	
I	✓	✓			$\Delta k_{FT,AB} = k_{1140,\text{nonuniform AB}} - k_{ref}$
II	✓		✓		$\Delta k_{FT,AM} = k_{1140,\text{nonuniform AM}} - k_{ref}$
III	✓			✓	$\Delta k_{FT,CB} = k_{1140,\text{full insertion}} - k_{ref}$
IV		✓	✓		$\Delta k_{AB,AM} = k_{\text{nonuniform AB,nonuniform AM}} - k_{ref}$
V		✓		✓	$\Delta k_{AB,CB} = k_{\text{nonuniform AB,full insertion}} - k_{ref}$
VI			✓	✓	$\Delta k_{AM,CB} = k_{\text{nonuniform AM,full insertion}} - k_{ref}$

AB, axial burnup profile; AM, axial moderator density profile; CB, control blade usage; FT, fuel temperature.

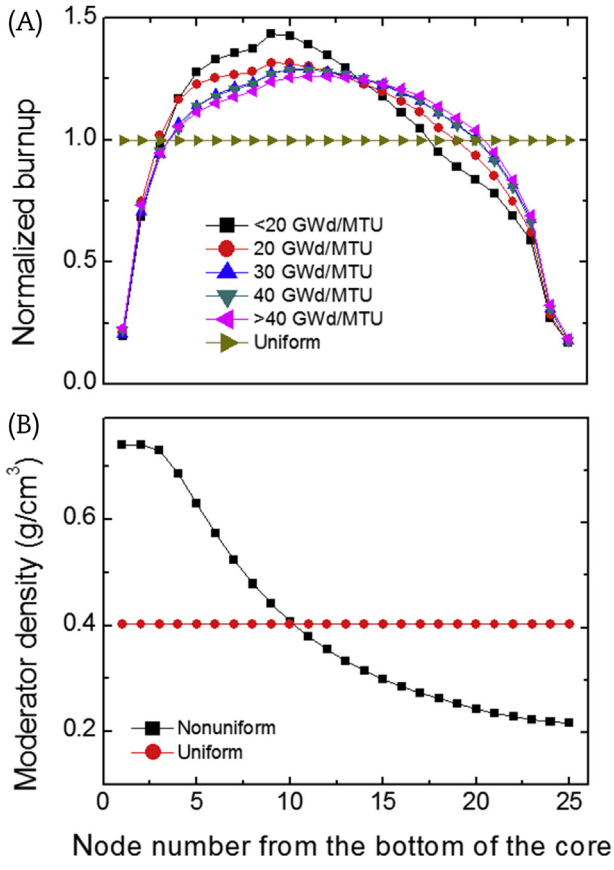

Fig. 2. Uniform and nonuniform profiles. (A) Axial burnup profile. (B) Axial moderator density profile.

3. Results

Before exploring these compound effects, however, an explanation of the mechanisms of how Δk varies with the four single effects is essential. First, an increase of FT during power operation increases the Doppler broadening effect in ^{238}U resonances. Hence, there is an increase in the absorption of epithermal neutrons in ^{238}U, followed by an increase in plutonium generation [2] as well as in the magnitude of k_{eff} in spent fuel assemblies. Two examples are given as follows: Δk_{FT} is calculated and found to be 57 and 690 pcm when $B = 10$ and 50 GWd/MTU, respectively. Notably, for simplicity, the FT adopted in this study was assumed to be axially uniform, which was different from the actual temperature, which varies axially during real power operation. However, the Δk between the cases of using uniform and nonuniform FT profiles has been proved to be less than 0.1% Δk [9]. Hence, the utilization of a uniform FT profile during power operation is appropriate.

Second, during power operation, the center region of the fuel assembly is the most reactive part due to neutron leakage at both the bottom and the top [6]. That is, there is lower burnup near the ends of the fuel assemblies. Furthermore, because of the inverse nature of reactivity effects on the remaining fissile nuclides, the regions near the ends of the fuel assemblies control the reactivity when the fuel assemblies are in storage [10]. This phenomenon is enhanced for nonuniform (i.e., other than flat) ABs in higher burnup conditions [6]. Hence, the magnitude of k_{eff} in the spent fuel assemblies increases accordingly. Two examples are given as follows: k_{AB} is calculated and found to be 921 and 14,641 pcm when $B = 10$ and 50 GWd/MTU, respectively. Notably, for simplicity, all the operating parameters were considered separately in this study. The variation of AB due to the AM or the insertion of the control blade during power operation was neglected. In addition, the ABs employed in this study were based on end-of-life profiles, so the variation of the burnup profile that occurs per cycle was not considered.

Third, similar to the reactivity in the AB mentioned above, the reactivity in the spent fuel assemblies is primarily due to the ends of the fuel assemblies. However, as shown in Fig. 2, the nonuniform AM in the fuel assemblies during power operation is bottom-peaked. Therefore, the top region of the fuel assemblies has a lower moderator density, resulting in a harder neutron energy spectrum and subsequently an increase of plutonium generation [6]. As a result, the magnitude of k_{eff} in the spent fuel assemblies increases and is larger than that when a uniform axial moderator density is used. Two examples are given as follows: Δk_{AM} is calculated and found to be 33 and 1,418 pcm when $B = 10$ and 50 GWd/MTU, respectively.

Fourth, using a control blade in a BWR during power operation tends to harden the neutron energy spectrum, resulting in an increase of plutonium generation [11]. Hence, an increase of plutonium nuclides tends to increase the magnitude of k_{eff} in the spent fuel assemblies. Two examples are given as follows: Δk_{CB} is calculated and found to be 437 and 5,777 pcm when $B = 10$ and 50 GWd/MTU, respectively.

Δk versus B for six types of compound effects and the values of Δk at 10 and 50 GWd/MTU for all the single and compound effects are shown in Fig. 3A–F and Table 3, respectively. Fig. 3B and C illustrate, respectively, Δk versus B for the compound effects of type II (FT, AM) and type III (FT, CB). As seen in Fig. 3B, the curve of $\Delta k_{FT,\,AM}$ versus B is almost the same as that of $\Delta k_{FT} + \Delta k_{AM}$ versus

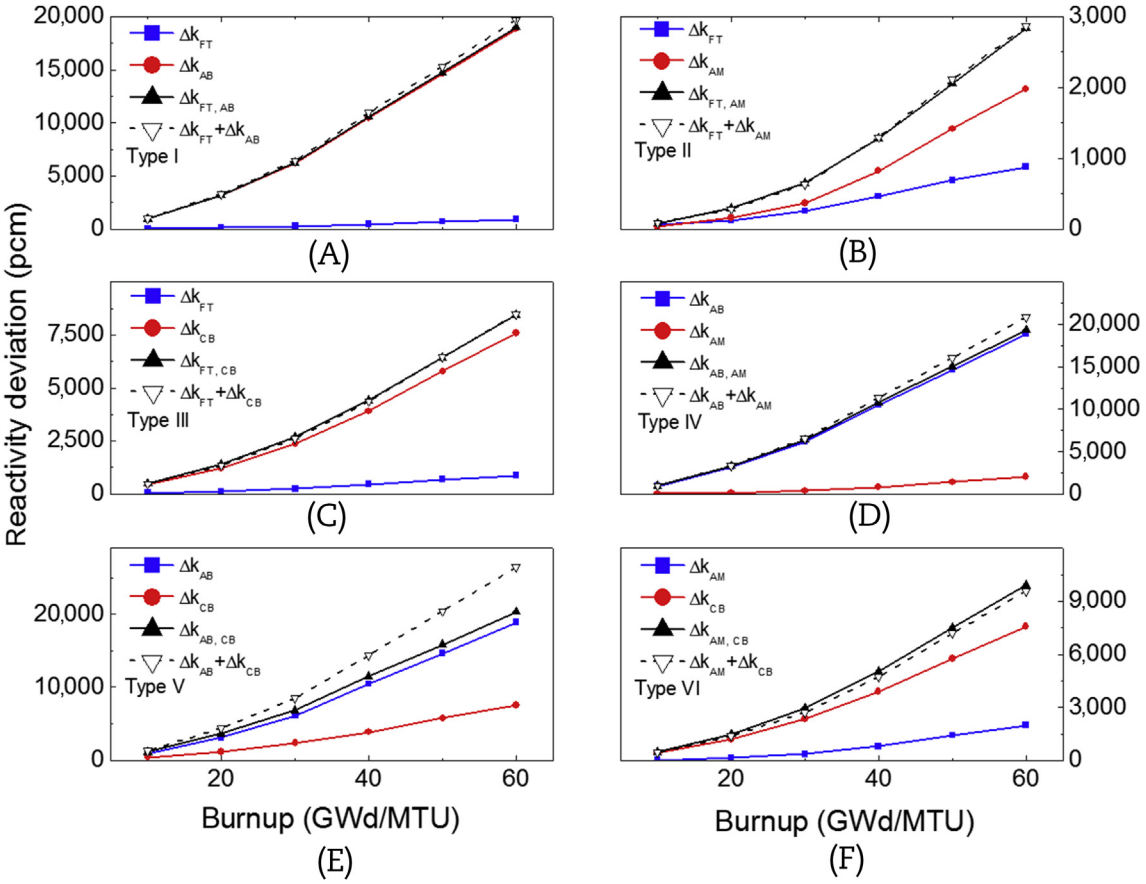

Fig. 3. Reactivity deviation versus burnup caused by single and compound effects. (A) FT, AB, and Type I. (B) FT, AM and Type II. (C) FT, CB and Type III. (D) AB, AM and Type IV (E) AB, CB and Type V (F) AM, CB and Type VI.

Table 3
Values of reactivity deviation for single and compound effects at two burnup levels of 10 and 50 GWd/MTU.

Δk (pcm)	Burnup (GWd/MTU)	
	10	50
Δk_{FT}	57	690
Δk_{AB}	921	14,641
Δk_{AM}	33	1,418
Δk_{CB}	437	5,777
$\Delta k_{FT,AB}$	940	14,749
$\Delta k_{FT,AM}$	85	2,055
$\Delta k_{FT,CB}$	509	6,438
$\Delta k_{AB,AM}$	964	15,024
$\Delta k_{AB,CB}$	1,193	15,876
$\Delta k_{AM,CB}$	500	7,522

B. This is also true in Fig. 3C. That is, the curve of $\Delta k_{FT,CB}$ versus B is also very close to the curve of $\Delta k_{FT} + \Delta k_{CB}$ versus B. In other words, the fact that the operating parameter of FT acts on $\Delta k_{FT,AM}$ or $\Delta k_{FT,CB}$ is independent of either AM or CB, respectively, and vice versa. When B = 10 GWd/MTU, $\Delta k_{FT,AM}$, Δk_{FT}, and Δk_{AM} are calculated and found to be 85, 57, and 33 pcm, respectively, while $\Delta k_{FT,CB}$, Δk_{FT}, and Δk_{CB} are 509, 57, and 437 pcm, respectively. Furthermore, for B = 50 GWd/MTU, $\Delta k_{FT,AM}$, Δk_{FT}, and Δk_{AM} are calculated and found to be 2,055, 690, and 1,418 pcm, respectively, while $\Delta k_{FT,CB}$, Δk_{FT}, and Δk_{CB} are 6,438, 690, and 5,777 pcm, respectively.

However, the results depicted in Fig. 3A–F, but not including Fig. 3B and C, show a significant discrepancy between the curve of Δk versus B resulting from the compound effects and the summation curve resulting from their two associated single effects. Such a Δk discrepancy increases as B increases. Shown in Fig. 3A and E are, respectively, Δk versus B for the compound effects of type I (FT, AB) and type V (AB, CB). As it can be seen, the curves of both $\Delta k_{FT,AB}$ versus B and $\Delta k_{AB,CB}$ versus B lie below those of $\Delta k_{FT} + \Delta k_{AB}$ and $\Delta k_{AB} + \Delta k_{CB}$, respectively. In particular, such Δk discrepancy increases as B increases, especially in regard to the compound effects of type V. As for the compound effects of type I, an increase in FT during power operation leads to an increase of plutonium generation, especially in the center region of the fuel assemblies. However, the utilization of nonuniform ABs during power operation tends to burn the fissile nuclides primarily in the center region, thus, leaving the regions near the ends of the fuel assemblies to control reactivity when the fuel assemblies are in storage. The fact that the latter effect counterbalances the former to some extent accounts for the reduction of Δk in the corresponding compound effects. For example, $\Delta k_{FT,AB}$, Δk_{FT}, and Δk_{AB} are, respectively, 940, 57, and 921 pcm when B = 10 GWd/MTU; these values can be compared to the values 14,749, 690, and 14,641 pcm when B = 50 GWd/MTU. Similarly, for type V compound effects, using the control blade during power operation leads to a harder neutron energy spectrum and subsequently an increase of plutonium generation. In addition, a greater amount of plutonium nuclides exist in the most reactive region (i.e., the center region) than in those regions near the ends of the fuel assemblies. As mentioned above, the nonuniform AB tends to burn the fissile nuclides, primarily in the center region, and this subsequently leads to greater consumption of plutonium there. Hence, Δk in the corresponding compound effects

is reduced. For example, $\Delta k_{AB,CB}$, Δk_{AB}, and Δk_{CB} are calculated and found to be 1,193, 921, and 437 pcm, respectively, when $B = 10$ GWd/MTU; however, these values are 15,876, 14,641, and 5,777 pcm when $B = 50$ GWd/MTU. Notably, if the variation of the axial power and burnup profiles due to control blade insertion is considered, the nonuniform AB is expected to shift axially up the fuel assembly. The most reactive region would not contain the greatest amount of plutonium nuclides, so Δk would not be the same as the value described above.

Fig. 3D shows Δk versus B for the compound effects of type IV (AB, AM). As can be seen, the curve of $\Delta k_{AB,AM}$ versus B lies above that of $\Delta k_{AB} + \Delta k_{AM}$ when B is less than 20 GWd/MTU [12]. The opposite is true when B is greater than 20 GWd/MTU. The reason for this is that, during power operation, the bottom-peaked AM results in a lower moderator density in the top region of the fuel assembly, which subsequently leads to an increase of plutonium generation. This phenomenon is enhanced when B is less than 20 GWd/MTU, at which point the AB is bottom-peaked. Hence, it results in a positive Δk discrepancy between the compound effects and the two associated single effects. Conversely, a negative Δk produces as the AB becomes center-peaked when B exceeds 20 GWd/MTU. For example, $\Delta k_{AB,AM}$, Δk_{AB}, and Δk_{AM} are calculated and found to be 964, 921, and 33 pcm, respectively, when $B = 10$ GWd/MTU; however, these values are 15,024, 14,641, and 1,418 pcm when $B = 50$ GWd/MTU.

Fig. 3F shows Δk versus B for the compound effects of type VI (AM, CB). As can be seen, the curve of $\Delta k_{AM,CB}$ versus B lies above that of $\Delta k_{AM} + \Delta k_{CB}$. As mentioned above, CB tends to harden the neutron energy spectrum during power operation, which subsequently leads to an increase of plutonium generation. This increase is enhanced by using the bottom-peaked axial moderator density. This is because that the top region of the fuel assemblies contains a lower moderator density, and so a harder neutron energy spectrum results. For example, $\Delta k_{AM,CB}$, Δk_{AM}, and Δk_{CB} are calculated and found to be 500, 33, and 437 pcm, respectively, when $B = 10$ GWd/MTU; however, these values are 7,522, 1,418, and 5,777 pcm when $B = 50$ GWd/MTU.

Fig. 4A shows Δk versus B only in the presence of major actinides (namely, "set α" hereafter) for four single effects. As can be seen, the set α resulting from all four single effects makes significant and positive contributions to Δk. The Δk resulting from the four single effects ranges from smallest to largest according to FT, AM, CB, and AB and increases as B increases. This phenomenon is primarily due to the fact that more fissile nuclides such as plutonium are generated as B increases. Fig. 4B shows the value of Δk versus B contributed by the minor actinides plus the major fission products (namely, "set β" hereafter) for four single effects. Only the set β resulting from the single effects of AB makes significant positive contributions to Δk. The resulting Δk also increases as B increases but is smaller than the value caused by set α when B exceeds 20 GWd/MTU. The single effects of CB, FT, and AM make only slight contributions to Δk and vary irregularly with B. In general, most of their contributions are negative. This phenomenon is mainly due to the hardening of the neutron energy spectrum and the subsequently lower amounts of minor actinides and because major fission products are consumed via neutron absorption. Notably, the energy-dependent fission yields of the fissile nuclides act as additional factors affecting the production of major fission products, and also, accordingly, Δk. In total, the Δk values resulting from the four single effects range from smallest to largest according to FT, AM, CB, and AB and increase as B increases.

Fig. 5A–F show Δk versus B caused by set α and set β for six types of compound effects. Fig. 5B and C illustrate Δk versus B caused by set α and set β for the compound effects of types II and III, respectively. In Fig. 5B, the resultant curves of Δk resulting from the

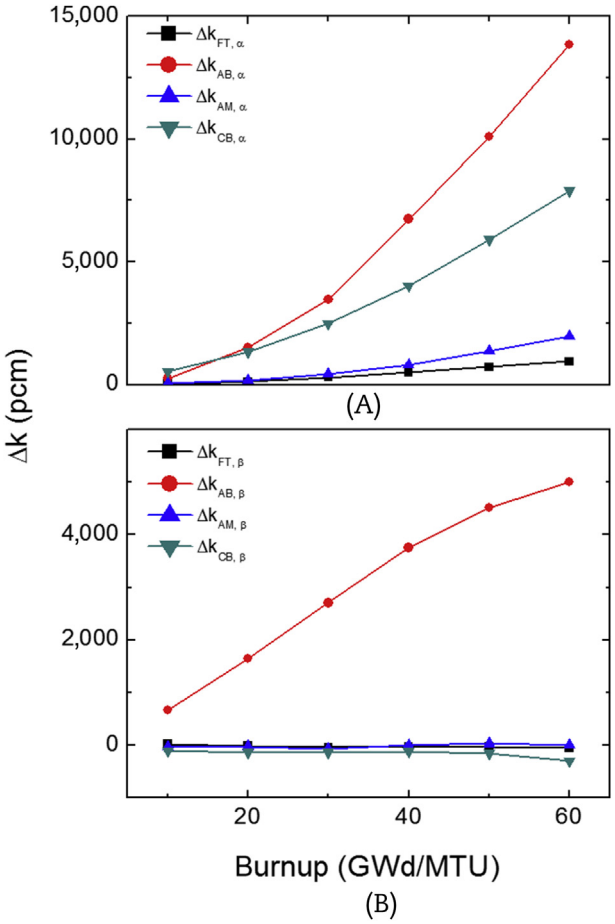

Fig. 4. Δk versus B caused by (A) set α and (B) set β for four single effects.

compound effects of type II are almost the same as a summation of the curves of Δk resulting from the two associated single effects for both set α and set β. This is also true in Fig. 5C. In other words, the way in which the operating parameter of the FT acts on Δk caused by either set α or set β is independent of either AM or CB.

Fig. 5A and D–F show a distinct discrepancy between the curve of Δk versus B resulting from the compound effects and a summation of the curves of Δk resulting from the two associated single effects caused by set α. However, only a slight Δk discrepancy is apparent in the one caused by set β. Fig. 5A and E illustrate, respectively, Δk versus B caused by set α and by set β for the compound effects of types I and V. For set α, the resultant curves of Δk due to the compound effects of both types I and V lie below a summation of the curves of Δk resulting from the two associated single effects. In addition, this sort of Δk discrepancy increases as B increases, especially in regard to type V compound effects. The reasons for this phenomenon closely correspond to those described in Fig. 3A and E. For set β, the resultant curve of Δk due to the type I compound effects nearly equals a summation of the curves of Δk resulting from the two associated single effects. However, the resultant curve of Δk resulting from the compound effects of type V is smaller than a summation of the curves of Δk resulting from the two associated single effects. This is mainly due to variation in the generation of major fission products, which is caused by the energy-dependent fission yields of the fissile nuclides.

Fig. 5D displays Δk versus B caused by set α and set β for the compound effects of type IV. For set α, the resultant curve of Δk resulting from the compound effects lies below a summation of the

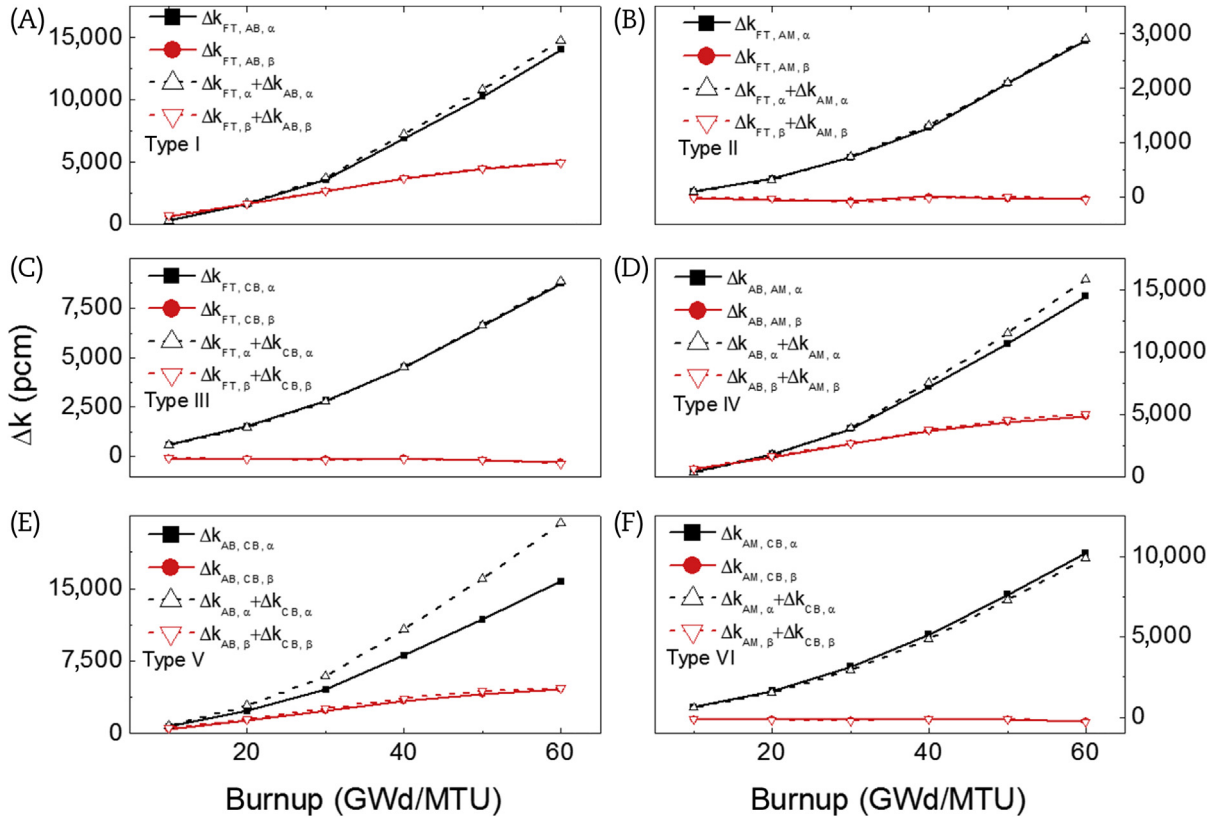

Fig. 5. Δk versus B caused by sets α and β for six types of compound effects. (A) Type I. (B) Type II. (C) Type III. (D) Type IV. (E) Type V. (F) Type VI.

curves of Δk resulting from the two associated single effects when B exceeds 30 GWd/MTU. However, for set β, the resultant curve of Δk resulting from the compound effects lies below a summation of the curves of Δk resulting from the two associated single effects. In total, the resultant curve of Δk resulting from the compound effects lies below a summation of the curves of Δk resulting from the two associated single effects when B exceeds 20 GWd/MTU, corroborating the results depicted in Fig. 3D.

Fig. 5F displays Δk versus B caused by set α and set β for the compound effects of type VI. For set α, the resultant curve of Δk resulting from the compound effects lies above a summation of the curves of Δk resulting from the two associated single effects. However, this Δk discrepancy increases only slightly as B increases. For set β, the resultant curve of Δk resulting from the compound effects is nearly equal to a summation of the curves of Δk resulting from the two associated single effects. Finally, from the results of Fig. 5A–F, it can be summarized that the Δk discrepancy between the compound effects and the two associated single effects is mainly caused by set α.

To simplify the burnup credit analysis, a general formula to express k_{eff} versus B for both single and compound effects is necessary. Since k_{eff} can be approximated by a first degree polynomial of B, in this study, the general formula is proposed as follows:

$$k_{\text{eff}} = mB + k_0 \tag{1}$$

where, m denotes the slope and k_0 represents the offset value of 0.99041, indicating the k_{eff} value for the fresh fuel assemblies ($B = 0$) in the cask. In this study, the magnitudes of m for all four single effects were obtained by least-squares fitting of Eq. (1) to the calculated results. Furthermore, the magnitude of m for the compound effects was obtained by carrying out a linear regression and fitting analysis. The final formula is given as follows:

$$m = -0.003325 c_{\text{AB}}(c_{\text{FT}} + c_{\text{AM}} c_{\text{CB}}) \tag{2}$$

where, c_{AB}, c_{FT}, c_{AM}, and c_{CB} denote the coefficients in relation to the operating parameters AB, FT, AM, and CB, respectively, and are fitted to values of 0.5805, 0.9639, 0.9218, and 0.6692. As for the single effects, only one out of these four coefficients (i.e., the one that is the associated operating parameter under investigation) is used; the other three are set at 1. Similarly, for the compound effects, only two out of the four coefficients (i.e., the two associated operating parameters under investigation) are used; the other two are set at 1. Fig. 6A–F show, respectively, a comparison of the calculated results, fitting curve, and Eq. (1) for the compound effects of types I to VI. As can be clearly seen, the results of the fitting curve and of Eq. (1) are in close agreement.

4. Discussion

This study carried out a series of calculations and analyses to evaluate the impact of single and compound effects on burnup credit of BWR spent fuel assemblies. It was found that Δk, resulting from either single or compound effects, increases as B increases. The magnitude of the resultant Δk due to four single effects ranges from smallest to largest according to FT, AM, CB, and AB. The contributions to Δk are mainly caused by the major actinides for all four single effects, with the exception of the value of Δk resulting from AB, as B is less than 20 GWd/MTU, which is primarily due to the contributions of major fission products.

Furthermore, only Δk values resulting from either type II or III compound effects can be approximated using a summation of the

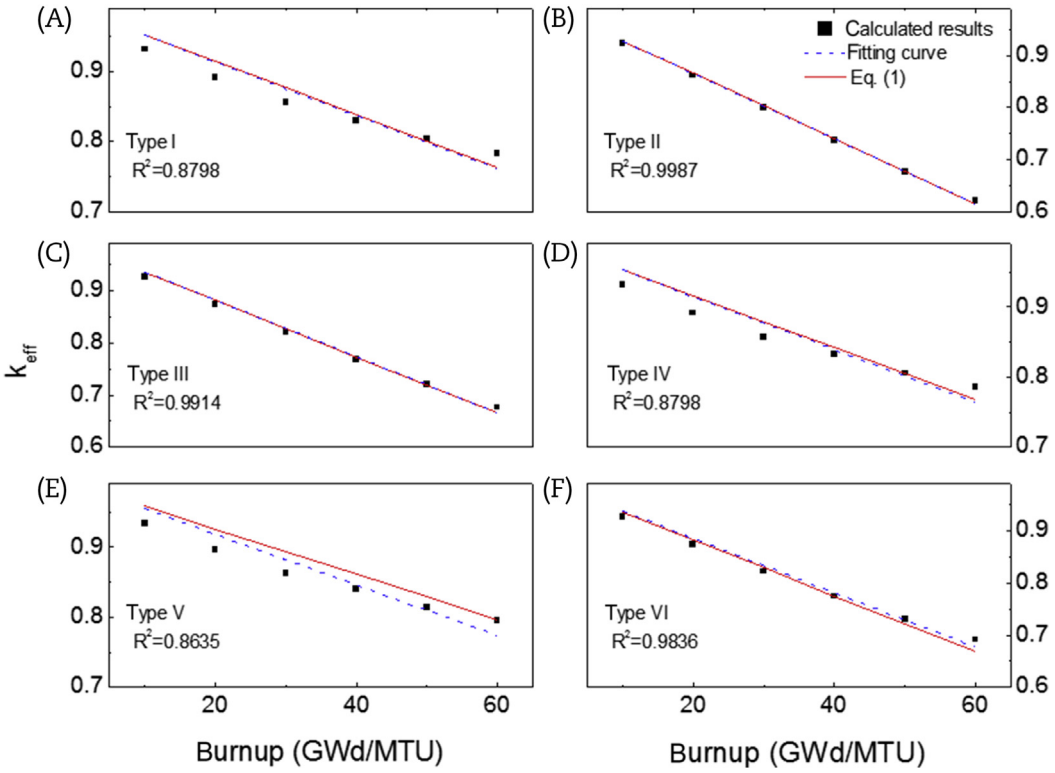

Fig. 6. Comparison of calculated results, fitting curves, and Eq. (1) for various compound effects. (A) Type I. (B) Type II. (C) Type III. (D) Type IV. (E) Type V. (F) Type VI.

values resulting from the two associated single effects. The Δk resulting from either type I or V compound effects is smaller than a summation of the values resulting from the two associated single effects. However, the opposite is true for type VI compound effects. When B is less than 20 GWd/MTU, the value of Δk resulting from type IV compound effects is larger than a summation of the values resulting from the two associated single effects However, the opposite is true when B is greater than 20 GWd/MTU. In general, the Δk discrepancy between the compound effects and the two associated single effects increases as B increases, especially for type V compound effects. In addition, such Δk discrepancy ranges from smallest to largest according to types II, III, VI, I, IV, and V.

Finally, this study has successfully proposed a general formula to express k_{eff} versus B for both single and compound effects. Such a formula can greatly facilitate burnup credit analysis. However, this study presents only a general approach to investigating the compound effects of the operating parameters on the burnup credit of spent fuel. The conditions of the operating parameters for the calculations were determined only based on simplified assumptions. Therefore, further investigation on the complex operating parameters (e.g., the incorporation of Gd rods or partial-length fuel rods), more realistic operating conditions (e.g., the consideration to partial insertion of control blade or operating history), or other types of spent fuel should be conducted for precise estimates of the burnup credit in spent fuel.

Conflicts of interest

All authors declare there is no conflicts of interest.

References

[1] D.E. Mueller, J.M. Scaglione, J.C. Wagner, S.M. Bowman, Computational Benchmark for Estimated Reactivity Margin from Fission Products and Minor Actinides in BWR Burnup Credit, NUREG/CR-7157, ORNL/TM-2012/96, U.S. Nuclear Regulatory Commission, Oak Ridge National Laboratory, Oak Ridge (TN), 2012.

[2] D.E. Mueller, S.M. Bowman, W.(B.J.) Marshall, J.M. Scaglione, Review and Prioritization of Technical Issues Related to Burnup Credit for BWR Fuel, NUREG/CR-7158, ORNL/TM-2016/261, U.S. Nuclear Regulatory Commission, Oak Ridge National Laboratory, Oak Ridge (TN), 2012.

[3] W.(B.J.) Marshall, B.J. Ade, S.M. Bowman, I.C. Gauld, G. Ilas, U. Mertyurek, G. Radulescu, Technical Basis for Peak Reactivity Burnup Credit for BWR Spent Nuclear Fuel in Storage and Transportation Systems, NUREG/CR-7194, ORNL/TM-2014/240, U.S. Nuclear Regulatory Commission, Oak Ridge National Laboratory, Oak Ridge (TN), 2015.

[4] G. You, C. Zhang, X. Pan, Introduction of burn-up credit in nuclear criticality safety analysis, Proc. Eng. 43 (2012) 297–301.

[5] J.C. Wagner, M.D. DeHart, B.L. Broadhead, Investigation of Burnup Credit Modeling Issues Associated with BWR Fuel, ORNL/TM-1999/193, U.S. Nuclear Regulatory Commission, Oak Ridge National Laboratory, Oak Ridge (TN), 2000.

[6] J.C. Wagner, M.D. DeHart, Review of Axial Burnup Distribution Considerations for Burnup Credit Calculations, ORNL/TM-1999/246, Oak Ridge National Laboratory, Oak Ridge (TN), 2000.

[7] ORNL, SCALE: A Comprehensive Modeling and Simulation Suite for Nuclear Safety Analysis and Design, ORNL/TM-2005/39, Version 6.1, Oak Ridge National Laboratory, Oak Ridge (TN), 2011.

[8] D.P. Henderson, Summary Report of Commercial Reactor Criticality Data for LaSalle Unit 1, B00000000-B00001717-57015-00138 REV 00, CRWMS/M&O, Las Vegas (NV), 1999.

[9] B.J. Ade, W.(B.J.) Marshall, G. Ilas, B.R. Betzler, S.M. Bowman, Impact of Operating Parameters on Extended BWR Burnup Credit, ORNL/TM-2017/46, U.S. Nuclear Regulatory Commission, Oak Ridge National Laboratory, Oak Ridge (TN), 2017.

[10] NEI, Guidance for Performing Criticality Analyses of Fuel Storage at Light-Water Reactor Power Plants, NEI 12–16, Revision 1, Nuclear Energy Institute (NEI), Washington D.C., 2014.

[11] W.(B.J.) Marshall, B.J. Ade, S. Bowman, J.S. Martinez-Gonzalez, Axial Moderator Density, Control Blade Usage, and Axial Burnup Distributions for Extended BWR Burnup Credit, NUREG/CR-7224, ORNL/TM-2015/544, U.S. Nuclear Regulatory Commission, Oak Ridge National Laboratory, Oak Ridge (TN), 2016.

[12] S.C. Wu, D.S. Chao, J.H. Liang, Parametric study of the burnup credit criticality analysis in BWR fuels, 24th International Conference on Nuclear Engineering (24th ICONE), Charlotte (NC), June 26–30, 2016.